STEM CELLS®

TISSUE-SPECIFIC STEM CELLS

Cdk6-Dependent Regulation of G_1 Length Controls Adult Neurogenesis

PIERRE BEUKELAERS,[a,*] RENAUD VANDENBOSCH,[a,*] NICOLAS CARON,[a] LAURENT NGUYEN,[a] SHIBESHIH BELACHEW,[b] GUSTAVE MOONEN,[a,b] HIROAKI KIYOKAWA,[c] MARIANO BARBACID,[d] DAVID SANTAMARIA,[d] BRIGITTE MALGRANGE[a]

[a]GIGA-Neurosciences, University of Liège, Liège, Belgium; [b]Department of Neurology, C.H.U. Sart Tilman, Liège, Belgium; [c]Department of Molecular Pharmacology and Biological Chemistry, Northwestern University, Feinberg School of Medicine, Chicago, Illinois, USA, [d]Molecular Oncology Programme, Centro Nacional de Investigaciones Oncológicas, Melchor Fernández Almagro, Madrid, Spain

Key Words. Adult neurogenesis • Cell cycle • G_1 length • Cyclin-dependent kinase • Dentate gyrus • Subventricular zone

ABSTRACT

The presence of neurogenic precursors in the adult mammalian brain is now widely accepted, but the mechanisms coupling their proliferation with the onset of neuronal differentiation remain unknown. Here, we unravel the major contribution of the G_1 regulator cyclin-dependent kinase 6 (Cdk6) to adult neurogenesis. We found that Cdk6 was essential for cell proliferation within the dentate gyrus of the hippocampus and the subventricular zone of the lateral ventricles. Specifically, Cdk6 deficiency prevents the expansion of neuronally committed precursors by lengthening G_1 phase duration, reducing concomitantly the production of newborn neurons. Altogether, our data support G_1 length as an essential regulator of the switch between proliferation and neuronal differentiation in the adult brain and Cdk6 as one intrinsic key molecular regulator of this process. STEM CELLS *2011;29:713–724*

Disclosure of potential conflicts of interest is found at the end of this article.

INTRODUCTION

Brain plasticity is expressed in diverse manners in adulthood and includes de novo neuronal production. This evolutionary conserved process occurs at least in two specific compartments of the adult brain: the subgranular zone (SGZ) of the hippocampal dentate gyrus (DG) and the subventricular zone (SVZ) of the lateral ventricles whose neural precursor cells (NPC) give rise to dentate granule neurons and olfactory bulb (OB) interneurons, respectively [1]. Although much has been elucidated about the identity and fate of adult precursor cells, the mechanisms that couple proliferation with neuronal differentiation in the adult brain remain largely unknown.

During the cell cycle, G_1 is an essential phase in which there is integration and response to extracellular cues that either allow progression through the cell cycle or promote withdrawal from the cell cycle to embark on a differentiation pathway [2]. Progression through G_1 is driven by the concerted action of cyclin-dependent kinase (Cdk) 4 (Cdk4) and the closely-related Cdk6 and their activating partners, that is, the D-type cyclins [3]. Once activated by D-type cyclins, Cdk4/6 phosphorylate the retinoblastoma protein (pRb), leading pRb to release E2fs. E2fs are transcriptional activators that, once freed from pRb, are able to activate the transcription of genes necessary to enter S-phase [4, 5]. Conversely, Cdk4/6 activity is suppressed through interactions with members of two families of inhibitory proteins: the Ink4 proteins ($p15^{Ink4a}$, $p16^{Ink4b}$, $p18^{Ink4c}$, and $p19^{Ink4d}$) that exhibit selectivity for Cdk4/6, and the Cip/Kip proteins ($p21^{Cip1}$, $p27^{Kip1}$, and $p57^{Kip2}$) that have a broader range of Cdk inhibitory activity [6].

Recently, accumulating evidence ascribed crucial roles to regulators of Cdk4/6 activity in controlling adult neurogenesis. For instance, $p27^{Kip1}$ selectively constrains transit-amplifying cell proliferation in the SVZ [7], whereas deletion of Cyclin D2 virtually abrogates adult neurogenesis [8]. However, the direct and specific contribution of the catalytic partners Cdk4 and Cdk6 to adult neurogenesis has not been evaluated yet. Moreover, to date, no study reported how cell cycle and particularly G_1 parameters are affected in adult neural precursors following genetic ablation of G_1 regulators.

In this report, we used knockout mice for the G_1 regulators Cdk4 and Cdk6 to analyze their respective contribution to adult neurogenesis. We showed that Cdk6 specifically controls the expansion of neuronally committed precursors and their rate of cell cycle withdrawal by regulating the length of G_1. Thus, our study describes for the first time the importance

Author contribution: P.B. and R.V.: conception and design, collection and/or assembly of data, data analysis and interpretation, manuscript writing; N.C.: collection and/or assembly of data, data analysis and interpretation; L.N.: data analysis and interpretation, critical review of the manuscript; S.B. and G.M.: financial support, critical review of the manuscript; H.K. and M.B.: provision of study material; D.S.: provision of study material, conception and design, data analysis and interpretation, critical review of the manuscript; B.M.: conception and design, financial support, data analysis and interpretation, final approval of the manuscript.
*P.B. and R.V. contributed equally to this work.

Correspondence: Brigitte Malgrange, Ph.D., GIGA-Neurosciences, University of Liège, Avenue de l'Hôpital, 1 Bâtiment B36, +1, 4000 Liège, Belgium. Telephone: +32-4366-5905; Fax: +32-4366-5912; e-mail: bmalgrange@ulg.ac.be Received November 3, 2010; accepted for publication January 31, 2011; first published online in STEM CELLS *EXPRESS* February 11, 2011.
1066-5099/2009/$30.00/0 doi: 10.1002/stem.616

of regulating G_1 duration for fine-tuning neuronal production in the adult brain.

Materials and Methods

Animals

$Cdk4^{-/-}$ [9] and $Cdk6^{-/-}$ [10] colonies were maintained on a mixed CD1 × C57BL/6J × FVB × S129/sv and a mixed CD1 × C57BL/6J background, respectively. Wild type (WT) and knockout mice used in all experiments were obtained from heterozygous breedings and genotype was determined by polymerase chain reaction as described previously. Unless otherwise mentioned, 6-week-old male and female mice were used in all experiments. Mice were group-housed in the animal facility at the University of Liège under standard conditions with food and water ad libitum and were maintained on a 12-hour light/dark cycle. All animals were taken care of in accordance with the declaration of Helsinki and following the guidelines of the Belgian Ministry of Agriculture in agreement with European Community laboratory Animal Care and Use Regulations (86/609/CEE, Journal Officiel des Communautés Européennes number L358, 18 December 1986).

Seizure Induction

See Supporting Information.

BrdU Administration and Detection

See Supporting Information.

Immunofluorescence

Tissue was prepared as described in Supporting Information. All staining was performed on 40-μm free-floating sections. Sections underwent antigen retrieval for 30 minutes at 95°C in Target Retrieval Solution (Dako, Glostrup, Denmark), were then rinsed in Tris-buffered saline (TBS) and incubated overnight at 4°C with primary antibodies (complete list of primary antibodies as Supporting Information) diluted in TBS containing 0.1% Triton, 0.1% Tween 20 and 5% normal donkey serum (blocking solution). After washings in TBS, sections were incubated for 1 hour at room temperature in blocking solution containing the corresponding secondary antibodies (1:500, Jackson ImmunoResearch, Europe Ltd, Suffolk, U.K.), either coupled to Fluorescein Isothiocyanate (FITC), Rhodamine Red-X, or Cy5. Finally, sections were rinsed in TBS and mounted between slide and coverslide using VectaShield Hard Set mounting medium containing 4′,6-diamidino-2-phenylindole (DAPI) (Vector Laboratories, Burlingame, CA). The slides were stored in the dark at 4°C.

Confocal Microscopy

Fluorescence images were acquired using the Olympus Fluoview FV1000 confocal system equipped with the Olympus IX81 inverted microscope (Olympus Europa GmbH, Hamburg, Germany). Fields were acquired using Z-scan with a step of 1.5 μm between each confocal plane. All sections prepared for comparison were analyzed at the same time, using the same acquisition parameters.

Quantification of Cell Numbers

All quantifications were realized by an experimentator blind to the experimental conditions. To evaluate cell proliferation and neurogenesis in the DG, we counted exhaustively in the SGZ (SGZ + granule cell layer [GCL] for bromodeoxyuridine [BrdU] 4 weeks analysis), the number of Ki-67^+ or $BrdU^+$ cells per DG section under a 60× objective in a sampling of every sixth 40 μm thick coronal section (240 μm) along the rostro-caudal axis of the DG. Cell numbers were expressed as the number of cells per mm^3 of GCL. For the SVZ, whose volume directly depends on the size of the proliferating population, a sampling of every sixth 40 μm thick coronal section (240 μm) from the most rostral crossing of the corpus callosum to the start of the third ventricle (crossing of the anterior commissure) (i.e., 1.10 mm to 0.14 mm from bregma) was taken and used for cell quantifications, as described previously [11]. The number of Ki-67^+ cells per SVZ was then obtained by multiplying the results by six to provide an accurate estimation of the number of cells per SVZ, as previously performed [12–14].

Quantification of Double and Triple Labeled Cells

Analysis of double and triple labeled cells was completed using methods similar to Steiner et al. [15]. Briefly, 1-in-12 series of sections of each animal were double or triple labeled as described above. At least 200 randomly chosen Ki-67^+ cells within the SGZ or SVZ were analyzed for their coexpression of Ki-67 and markers for the different subpopulations of precursor cells (Fig. 4A and Supporting Information Fig. 4) using a confocal microscope. The percentage of Ki-67^+ that were positive for the marker was then multiplied by the number of proliferating Ki-67^+ cells of the corresponding animal previously established as described above. This calculation yielded an accurate estimation of the number of proliferating (i.e., Ki-67^+)/$marker^+$ cells per mm^3 of GCL and Ki-67^+/$marker^+$ per SVZ. For cell cycle exit experiments, at least 200 randomly chosen $BrdU^+$ cells within the SGZ/GCL or anterior rostral migratory stream (RMS) were analyzed for their coexpression of Ki-67.

Cell Cycle Kinetics

To calculate the total length of the cell cycle (T_C) and the length of S-phase (T_S), the mean labeling index (LI, representing the proportion of $BrdU^+$ cells to the number of proliferating, i.e., Ki-67^+, cells) was plotted as a function of time after application of BrdU (Fig. 6B). Ki-67 is expressed during all phases of the cell cycle, except G_0, which makes it an appropriate growth fraction (GF) marker [16, 17]. The GF (representing the proportion of proliferating cells) was determined as the maximum LI value attained for each genotype. T_C and T_S were determined using (a) y-intercept = GF × T_S/T_C and (b) time to reach maximum LI = $T_C - T_S$ [18]. Mitotic cells were identified using antiphosphohistone H3 antibodies (mitotic marker). The combined length of G_2 plus M phases (T_{G2+M}) was determined as the time required to label all mitotic (i.e., Ki-67^+/$phH3^+$) cells with BrdU [18]. The length of G_1 phase (T_{G1}) was computed using the equation $T_{G1} = T_C - (T_S + T_{G2+M})$, as shown previously [18].

Western Blotting

See Supporting Information.

Statistical Analysis

All numerical analysis were performed using GraphPad Prism software version four for Macintosh. Statistical analysis was performed using Student's t test or two-way analysis of variance (ANOVA) followed by a Bonferroni's post-test, depending on the data that were analyzed (see figure legends for details). Data are presented as mean with standard deviation of mean (Mean ± SD). All experiments were performed on four to six different animals per genotype. Differences were considered statistically significant at $p < .05$.

Results

Cdk4 and Cdk6 Are Expressed in SGZ and SVZ Precursors

A detailed analysis of the expression pattern of the G_1 regulators Cdk4 and Cdk6 in the neurogenic regions of the adult brain is lacking. Using confocal microscopy, we first showed that both Cdk4 and Cdk6 were expressed in the SGZ (Fig. 1) and SVZ (Supporting Information Fig. 1). We further

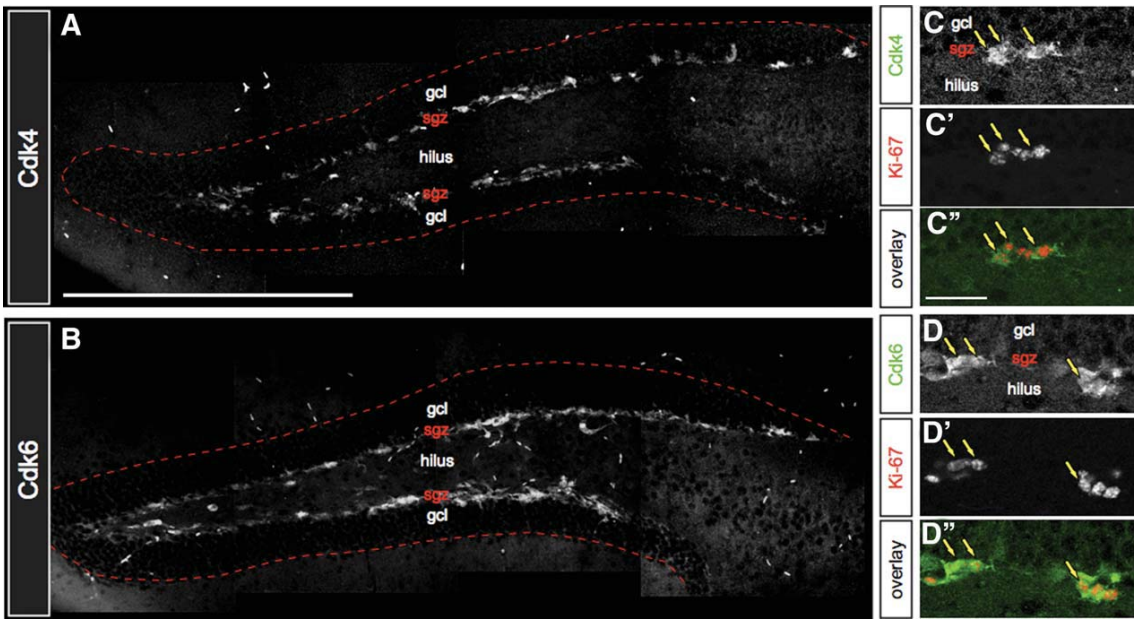

Figure 1. Expression pattern of cyclin-dependent kinase 4 (Cdk4) and Cdk6 in the dentate gyrus (DG). **(A, B):** Fluorescence images of sections of 6-week-old C57BL6/J DG stained with Cdk4 **(A)** and Cdk6 antibodies **(B)**. Red dashed lines indicate the outer boundary of the granule cell layer of the DG. Note that the labeling of both Cdks is restricted to the subgranular zone of the DG. **(C, D):** Fluorescence images of 1.5 μm thick confocal optical sections of DG stained with Cdk4 **(C)** and Ki-67 **(C′)** as well as Cdk6 **(D)** and Ki-67 **(D′)** antibodies. Respective overlays are in **(C″)** and **(D″)**. Yellow arrows point towards double labeled cells. Note the highly similar pattern between both Cdks and Ki-67. Scale bars = 420 μm **(A, B)**, 38 μm **(C–D″)**. Abbreviations: Cdk, cyclin-dependent kinase; gcl: granule cell layer; sgz: subgranular zone.

characterized the expression patterns of Cdk4 and Cdk6 by performing coimmunolabelings with antibodies directed against the proliferative marker Ki-67 (Fig. 1C, 1D). Confocal microscopy analysis revealed that virtually all Ki-67$^+$ cells in the SGZ expressed Cdk4 (95% ± 4.4%; $n = 3$) or Cdk6 (96% ± 2.8%; $n = 3$), suggesting that the overall majority of precursors express both Cdk4 and Cdk6. In agreement with these findings, we never detected any colabeling of Cdk4/6 with the postmitotic neuronal marker neuronal nuclei (NeuN) (Supporting Information Fig. 2), supporting that Cdk4/6 expression is restricted to proliferating cells in the adult brain.

Cdk6 Is Critical for Neural Precursor Proliferation in the SGZ and SVZ

The expression patterns of Cdk4 and Cdk6 in the SGZ and SVZ prompted us to hypothesize that these kinases could belong to the intrinsic mechanisms that underlie NPC proliferation in these neurogenic niches. As most Cdk4$^{-/-}$ mice survive until adulthood [9, 19] and Cdk6$^{-/-}$ develop normally [10], we took advantage of these genetic models to examine the contribution of Cdk4/6 to adult NPC proliferation. In agreement with previous studies reporting the dwarfism-like phenotype of Cdk4-deficient mice [9, 19], we first observed that Cdk4$^{-/-}$ brains were smaller and lighter than their WT counterparts at every postnatal stage analyzed, suggesting an important role for Cdk4 during brain development (Supporting Information Fig. 3). On the other hand, Cdk6$^{-/-}$ brains were hardly distinguishable from WT brains, although they displayed a small but significant reduced weight starting from postnatal day 30 (P30) (Supporting Information Fig. 3). To determine the importance of Cdk4/6 in the control of cell proliferation in the SGZ and SVZ, we then quantified the number of actively dividing Ki-67$^+$ cells in Cdk4$^{-/-}$ and Cdk6$^{-/-}$ animals. Quantifications first demonstrated that the number of Ki67$^+$ cells in the SGZ and SVZ was similar between Cdk4$^{-/-}$ and their respective WT littermates (Fig. 2A–2C and Supporting Information Fig. 4). On the other hand, we found a twofold reduction in the number of Ki-67$^+$ cells in the SGZ and SVZ of Cdk6$^{-/-}$ animals (Fig. 2D–2F and Supporting Information Fig. 4). Importantly, a similar proliferation defect was observed in the brain of 10-week-old Cdk6$^{-/-}$ mice (data not shown). Of note, in accordance with previous work showing that the genetic background influences adult NPC proliferation [20], we observed that WT animals arising from Cdk4 and Cdk6 colonies depict different levels of proliferation (Fig. 2C, 2F). Finally, we showed that Cdk4 and Cdk6 proteins were expressed at similar levels in WT mice coming from Cdk4 and Cdk6 colonies, ruling out any putative contribution of the genetic background and relative Cdk4/6 expression levels to the phenotypic discrepancies observed between Cdk4$^{-/-}$ and Cdk6$^{-/-}$ animals (Supporting Information Fig. 5). Overall, these results demonstrate that although Cdk4 and Cdk6 are both expressed by SGZ and SVZ neural precursors, Cdk6 seems to be more essential to promote their proliferation.

To examine whether the defect in proliferation observed in Cdk6$^{-/-}$ neurogenic areas impairs neuronal cell production, the number of cells coexpressing doublecortin (DCX) and NeuN was quantified in the DG of WT and Cdk6$^{-/-}$ mice (Fig. 3A–3E). These cells are young postmitotic neurons arising from proliferating precursors and therefore represent an accurate indicator of the rate of neurogenesis in the adult hippocampus [21]. There was a reduced number of DCX$^+$/NeuN$^+$ cells (Fig. 3E) in the absence of Cdk6, which is consistent with the decreased levels of precursor cell proliferation (Fig. 2). Importantly, most newly generated DCX$^+$/NeuN$^+$ neurons undergo a selection process, during which they are

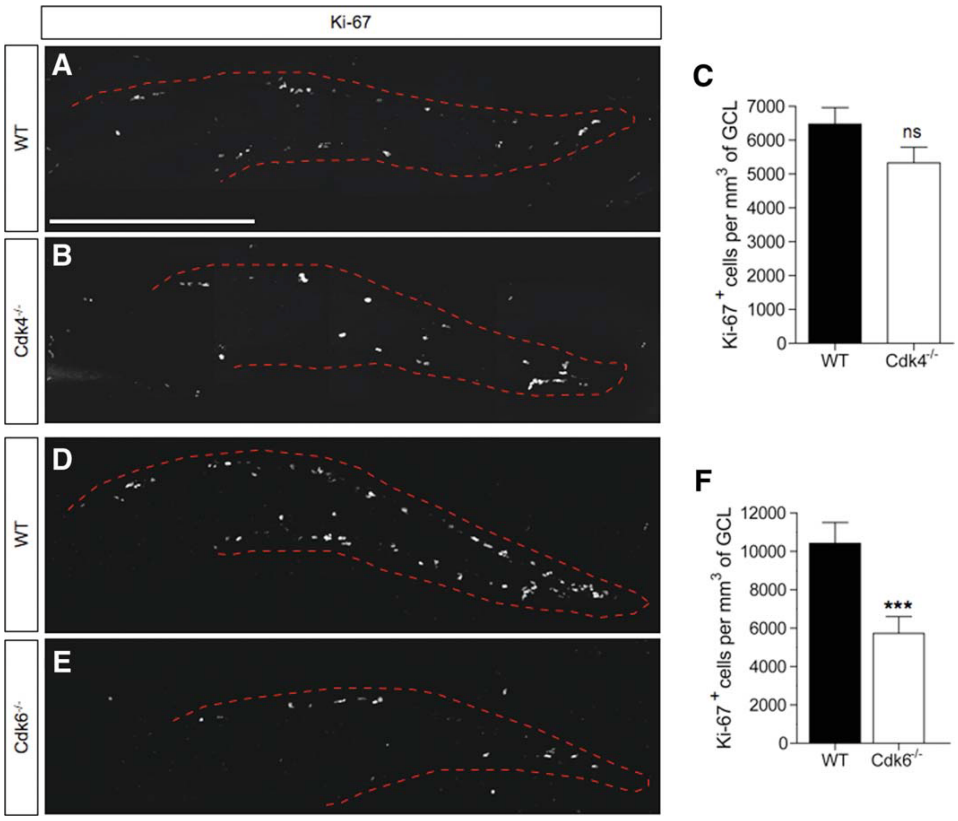

Figure 2. Cell proliferation in cyclin-dependent kinase (Cdk) $4^{-/-}$ and $Cdk6^{-/-}$ dentate gyrus (DG). **(A, B, D, E):** Fluorescence images of Ki-67 labeling in the DG of WT **(A)** and $Cdk4^{-/-}$ **(B)** as well as WT **(D)** and $Cdk6^{-/-}$ **(E)** mice. The red dashed lines delimitate the outer boundary of the granule cell layer (GCL). **(C, F):** Histograms showing the number of Ki-67^{+} cells per mm^3 of GCL of the DG in $Cdk4^{-/-}$ **(C)** and $Cdk6^{-/-}$ **(F)** brains when compared with their respective aged-matched WT littermates. Scale bar = 400 μm **(A, B, D, E)**. **(C, F):** Data are presented as mean ± SD and were analyzed by a Student's *t* test. *N* is five animals per condition. ***, $p < .001$. Abbreviations: Cdk, cyclin-dependent kinase; GCL, granule cell layer; WT, wild type; ns: not significant.

either recruited into function or eliminated, presumably by apoptosis [22]. Thus, we further analyzed whether Cdk6 deficiency affects the number of newborn neurons surviving in the DG. Hence, we injected BrdU once and quantified the number of $BrdU^{+}$ cells 4 weeks after the injection. We found a significant reduction of the number of surviving $BrdU^{+}$ cells in the Cdk6-deficient DG (Fig. 3J). Triple-labeling experiments of BrdU, NeuN, and astrocytic marker S100β showed that the vast majority of $BrdU^{+}$ cells became $NeuN^{+}$ neurons 4 weeks after birth regardless of the mouse genotype (Fig. 3F–3I for representative images in WT animals and Fig. 3K). Together with the reduced precursor proliferation and reduced $DCX^{+}/NeuN^{+}$ newborn neuron production, these data show that the absence of Cdk6 impedes long-lasting neuronal production in the DG. Similarly, the numbers of $BrdU^{+}/NeuN^{+}$ cells were reduced in the OB of mice deficient for Cdk6 4 weeks after the BrdU injection (data not shown). Finally, we sought to determine whether the lack of Cdk6 might affect the survival of newly born cells in the DG. Toward that purpose, we analyzed the expression of activated caspase3 in DG cells and compared the number of $BrdU^{+}/NeuN^{+}$ cells observed at 4 weeks to the number of $BrdU^{+}$ cells counted 2 hours after a single BrdU injection to obtain a survival ratio. Neither the number of cells undergoing apoptosis (Fig. 3L) nor the survival ratio (Fig. 3M) were found to be significantly different between WT and $Cdk6^{-/-}$ animals, suggesting that the net reduction of neuronal production observed in Cdk6-deficient mice does not result from impaired cell survival. Altogether, these data support that Cdk6 is central to adult neurogenesis by regulating the expansion of the precursor pool and hence newborn neuron production.

Cdk6 Selectively Regulates the Proliferation of Neuronally Committed Precursors of the DG

Several types of precursors can be identified in adult neurogenic niches according to their specific morphology and expression of unique sets of molecular markers [23] (Fig. 4A and Supporting Information Fig. 7). Previous works have demonstrated that cell cycle regulation in the adult brain is precursor-type-specific [24], thus we sought to determine whether the defect in proliferation observed in $Cdk6^{-/-}$ brains was restricted to a subpopulation versus all cycling precursors. First, we used glial fibrillary acidic protein (GFAP) and the Sry-related HMG box transcription factor Sox2 to identify immature DG precursors with, respectively, radial (type 1) and nonradial (type 2a) morphology that are not yet restricted to a neuronal fate [25]. No significant differences in the number of proliferating $GFAP^{+}$ (i.e., $GFAP^{+}/Ki\text{-}67^{+}$) nor $Sox2^{+}$ (i.e., $Sox2^{+}/Ki\text{-}67^{+}$) precursors were found in $Cdk6^{-/-}$ mice (Fig. 4B–4E). Neuronally committed precursors (types 2b and 3) were identified with antibodies against Neurod1 and DCX

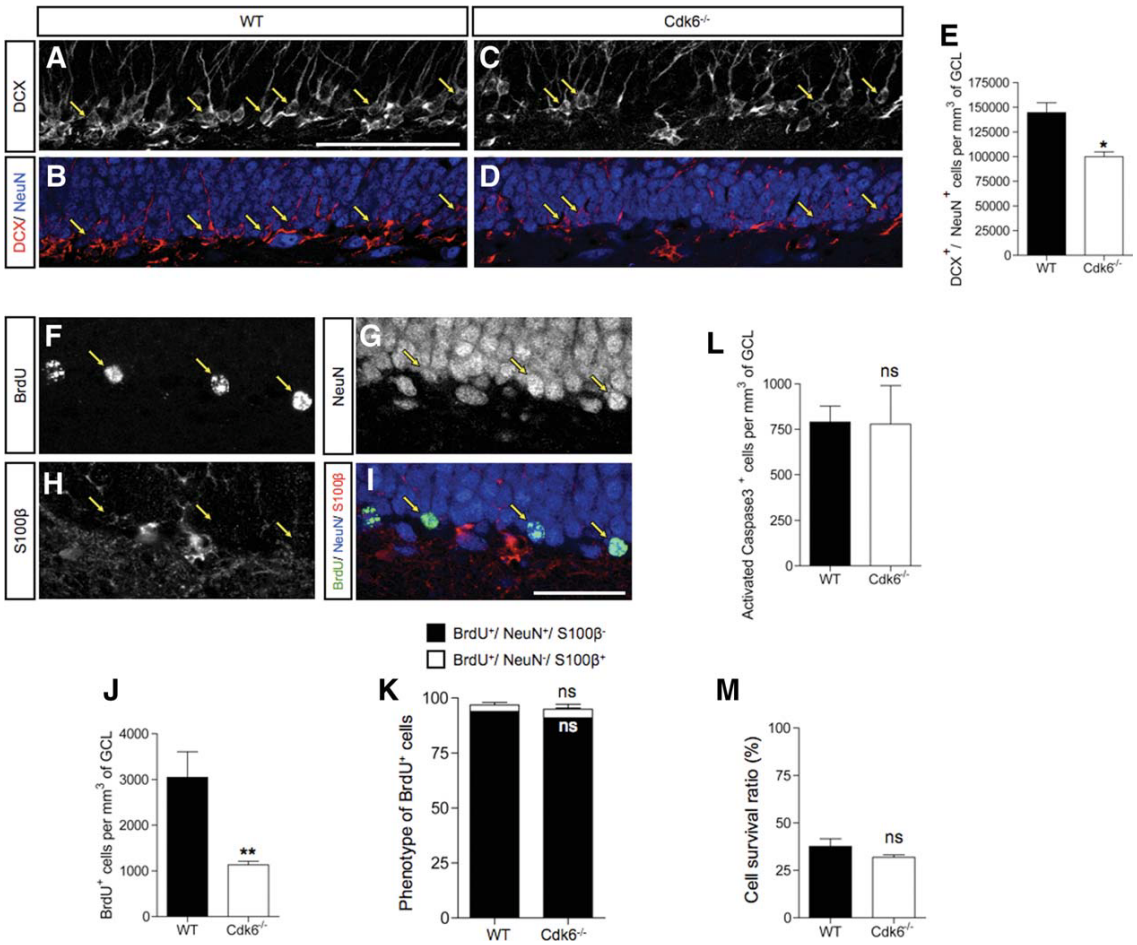

Figure 3. Neurogenesis in cyclin-dependent kinase (Cdk) $6^{-/-}$ dentate gyrus (DG). **(A–D):** Fluorescence images of DG stained with doublecortin (DCX) **(A, C)** and colabeled with NeuN **(B, D)** in WT **(A, B)** and Cdk6$^{-/-}$ **(C, D)** brains. Yellow arrows point toward DCX$^+$/NeuN$^+$ double labeled cells. **(E):** Histograms showing the number of DCX$^+$/NeuN$^+$ cells per mm^3 of granule cell layer (GCL) between WT and Cdk6$^{-/-}$ brains. **(F–I):** Fluorescence images of 1.5 μm thick confocal optical sections stained with BrdU **(F)**, NeuN **(G)**, S100β **(H)**, and respective overlays **(I)** 4 weeks after a single BrdU injection in WT animals. Yellow arrows point toward BrdU$^+$/NeuN$^+$/S100β^- cells. **(J):** Histograms showing the number of BrdU$^+$ cells per mm^3 of GCL 4 weeks after a single BrdU injection in WT and Cdk6$^{-/-}$ animals. **(K):** Histograms showing the percentage of BrdU$^+$ cells that were either NeuN$^+$/S100β^- or NeuN$^-$/S100β^+ (black- and white-filled portions of the histograms, respectively) 4 weeks after a single BrdU injection in WT and Cdk6$^{-/-}$ animals. Note that the vast majority of BrdU$^+$ became NeuN$^+$ (i.e., neurons) within 4 weeks, regardless of the genotype. **(L, M):** Histograms showing the number of activated caspase3$^+$ cells per mm^3 of GCL **(L)** and a BrdU cell survival ratio **(M)** (formula = #BrdU$^+$/NeuN$^+$ cells 4 weeks after a single BrdU injection/#BrdU$^+$ cells 2 hours after a single BrdU injection) in WT and Cdk6$^{-/-}$ animals. Scale bars = 105 μm **(A–D)**, 42 μm **(F–I)**. **(E, J, K, L, M):** Data are represented as mean ± SD and were analyzed by a Student's t test. N is four **(E)**, five **(J)**, five **(K)**, four **(L)**, and five **(M)** animals per condition. *, $p < .05$; **, $p < .005$. Abbreviations: BrdU, bromodeoxyuridine; Cdk, cyclin-dependent kinase; DCX, doublecortin; GCL, granule cell layer; NeuN, neuronal nuclei; ns: not significant; WT, wild type.

[26]. Quantifications revealed that the numbers of dividing precursors expressing these markers (i.e., Neurod1$^+$/Ki-67$^+$ and DCX$^+$/Ki-67$^+$) were all severely lowered in Cdk6$^{-/-}$ mice when compared with their WT littermates (Fig. 4F–4I). Consistently, we also observed that the numbers of neuronally committed precursors expressing Tbr2 (type 2b) [27] and the most committed Prox1-expressing precursor cells (type 3) [15] were reduced in the Cdk6$^{-/-}$ DG (Fig. 4J–4M). Finally, to address whether Cdk6 deficiency affects quiescent precursors of the SGZ, we first quantified the proportion of Sox2$^+$ cells that are negative for Ki-67 and detected no difference between WT and Cdk6$^{-/-}$ animals (Supporting Information Fig. 6). To further confirm this result, we tracked quiescent precursors by injecting BrdU twice a day for 1 week followed by a 28-day-chase before sacrifice (Supporting Information Fig. 6). We then counted the number of BrdU label-retaining quiescent precursors in the DG using BrdU/Sox2/S100β immunohistochemistry. In agreement with our previous data, no significant difference in the number of BrdU$^+$/Sox2$^+$/S100β^- cells was observed between WT and Cdk6$^{-/-}$ mice (Supporting Information Fig. 6). Altogether, these data support that Cdk6 is primarily involved in controlling the proliferation of neuronally committed precursors. We then defined whether Cdk6 deficiency would also preferentially affect the proliferation of a particular subpopulation of precursors of the SVZ. Using Sox2 as a marker of type B cells in the SVZ [28, 29], we first observed that the numbers of Sox2$^+$/Ki-67$^+$ cells were not impaired in the absence of Cdk6 (Supporting Information Fig. 7). SVZ type B cells continuously give rise to type C transit-amplifying cells themselves producing type A neuroblasts [30, 31] that migrate tangentially along the RMS to the OB, where they differentiate into GABAergic neurons

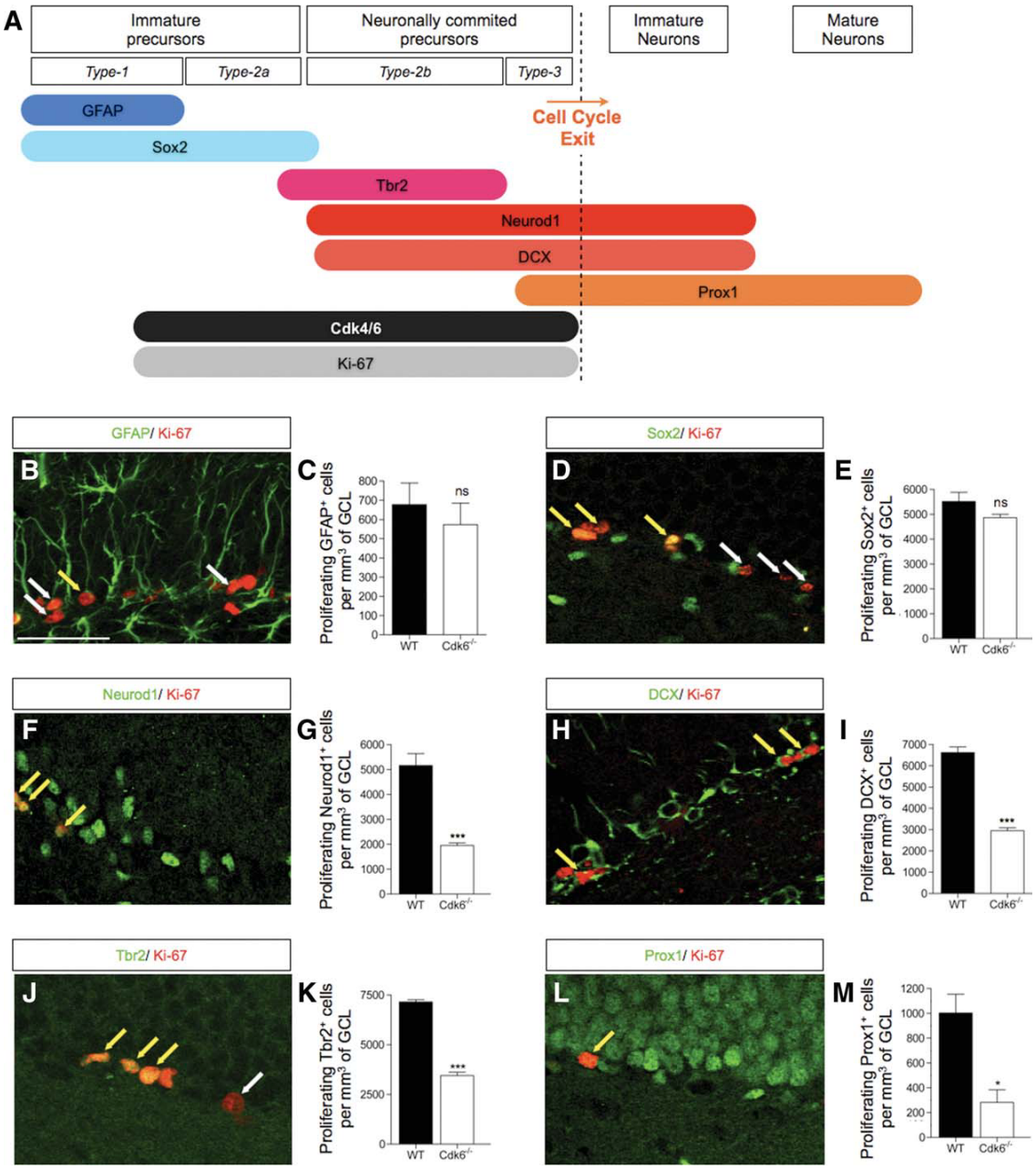

Figure 4. Subtype specific defect in cyclin-dependent kinase (Cdk) $6^{-/-}$ proliferating dentate gyrus (DG) precursors. **(A):** Milestones of neuronal development in the adult hippocampus. The expression pattern of Cdk4/6 is also displayed. **(B, D, F, H, J, L):** Fluorescence images of 1.5 μm thick confocal optical sections of DG costained with Ki-67 and glial fibrillary acidic protein (GFAP) **(B)**, Ki-67 and Sox2 **(D)**, Ki-67 and Neurod1 **(F)**, Ki-67 and doublecortin (DCX) **(H)**, Ki-67 and Tbr2 **(J)**, and Ki-67 and Prox1 **(L)** in WT animals. Yellow and white arrows represent double labeled Ki-67^{+}/$marker^{+}$ and single labeled Ki-67^{+}/marker-cells, respectively. **(C, E, G, I, K, M):** Histograms showing the number of proliferating (i.e., Ki-67^{+})/$GFAP^{+}$ **(C)**, Ki-67^{+}/ $Sox2^{+}$ **(E)**, Ki-67^{+}/$Neurod1^{+}$ **(G)**, Ki-67^{+}/DCX^{+} **(I)**, Ki-67^{+}/Tbr2 **(K)**, and Ki-67^{+}/Prox1 **(M)** cells per mm^3 of granule cell layer in WT and $Cdk6^{-/-}$ DG. Scale bar = 45 μm **(B, D, F, H, J, L)**. **(C, E, G, I, K, M):** Data are presented as mean ± SD and were analyzed by a Student's *t* test. *N* is four animals per condition. *, $p < .05$; ***, $p < .001$. Abbreviations: Cdk, cyclin-dependent kinase; DCX, doublecortin; GCL, granule cell layer; GFAP, glial fibrillary acidic protein; WT, wild type.

[32, 33]. To determine how critical Cdk6 is for the proliferation of these neuronally committed precursor populations, we quantified the numbers of $Dlx2^{+}$/DCX^{-}/Ki-67^{+} (type C) and $Dlx2^{+}$/DCX^{+}/Ki-67^{+} (type A) [34]. Both type C and type A proliferating precursors were reduced in the SVZ of $Cdk6^{-/-}$ mice (Supporting Information Fig. 7). Finally, we did not observe any defect in the number of BrdU label-retaining quiescent precursors in the SVZ (Supporting Information Fig. 6), suggesting that, similarly to the DG, Cdk6 principally controls the expansion of neuronally committed cells in the SVZ.

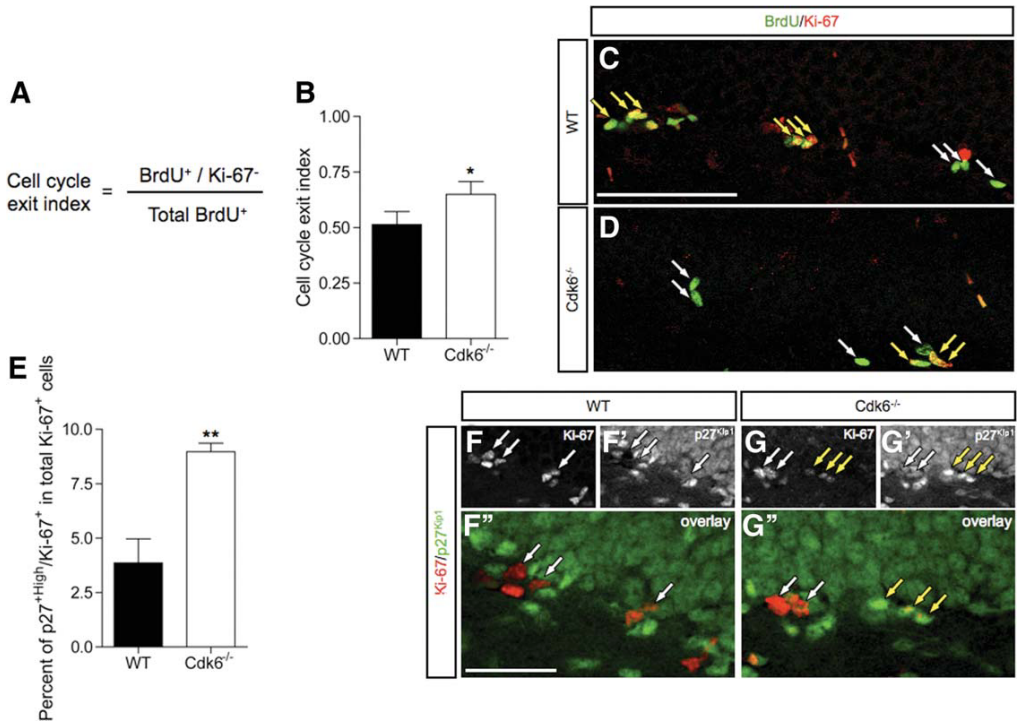

Figure 5. Cell cycle exit in cyclin-dependent kinase (Cdk) $6^{-/-}$ dentate gyrus (DG). **(A):** Ratio that was used to calculate the cell cycle exit index. **(B):** Histograms showing the cell cycle exit index in WT and $Cdk6^{-/-}$ DG precursors. **(C, D):** Representative images of 1.5 μm thick confocal optical sections of DG costained with Ki-67 and BrdU 24 hours after the injection. Yellow and white arrows in **(C, D)** represent $Ki\text{-}67^{+}$/$BrdU^{+}$ (i.e., cells that were incorporated BrdU 24 hours before sacrifice and either remained in the cell cycle or started a new cell cycle) and $Ki\text{-}67^{-}$/$BrdU^{+}$ (i.e., cells that incorporated BrdU and exited the cell cycle within the following 24 hours), respectively. **(E):** Histograms showing the percentage of $p27^{Kip1+High}$/$Ki\text{-}67^{+}$ in the total $Ki\text{-}67^{+}$ cells in WT versus $Cdk6^{-/-}$ subgranular zone. **(F–G″):** Fluorescence images of 1.5 μm thick confocal optical sections of DG costained with Ki-67 **(F, G)** and $p27^{Kip1}$ **(F′, G′)** and respective overlays **(F″, G″)** in WT **(F–F″)** and $Cdk6^{-/-}$ animals **(G–G″)**. White and yellow arrows in **(F–F″, G–G″)** represent $Ki\text{-}67^{+}$/$p27^{Kip1+Low}$ and $Ki\text{-}67^{+}$/$p27^{Kip1+High}$ cells, respectively. Scale bars = 70 μm **(C, D)**, 50 μm **(F″, G″)**, 100 μm **(F–F′, G–G′)**. Data are presented as mean ± SD and were analyzed by a Student's *t* test. **(B, E):** *N* is five **(B)** and four **(E)** animals per condition. *, $p < .05$; **, $p < .005$. Abbreviations: BrdU, bromodeoxyuridine; Cdk, cyclin-dependent kinase; WT, wild type.

$Cdk6^{-/-}$ Neural Precursors Prematurely Exit the Cell Cycle and Display a Lengthened G_1 Phase

It is currently assumed that neuronally committed precursors undergo a defined number of cell divisions before exiting the cell cycle and differentiating into neurons [26]. As these precursors give birth to postmitotic neurons, we hypothesized that the selective reduction of their pool could at least partially result from an enhanced rate of cell cycle exit. Hence, we injected mice with a single dose of BrdU, 24 hours before sacrifice. The cell cycle exit index was then scored by defining the ratio between $BrdU^{+}$/$Ki\text{-}67^{-}$ cells and total $BrdU^{+}$ cells in the DG, corresponding to the fraction of precursors leaving the cell cycle within 24 hours, as described previously [35–38] (Fig. 5A). The cell cycle exit index was significantly increased in $Cdk6^{-/-}$ (Fig. 5B–5D) but not $Cdk4^{-/-}$ (Cdk4WT: 47.88% ± 6.82%; $Cdk4^{-/-}$: 51.11% ± 2.73%; $p = .675$; $n = 4$) mice when compared with their respective age-matched WT littermates. Similarly, the cell cycle exit probability of future OB interneurons was increased in the anterior part of the RMS of $Cdk6^{-/-}$ animals (Supporting Information Fig. 8). It has been shown that the Cdk inhibitor $p27^{Kip1}$ progressively accumulates during G_1 phase in precursors as increased numbers of cell divisions occur [38, 39]. Using immunofluorescence, we distinguished two types of $p27^{Kip1+}$ cells in the DG, both of them exhibiting nuclear staining. Some cells predominantly found in the SGZ were strongly positive for $p27^{Kip1}$ (i.e., $p27^{Kip1+High}$), whereas others scattered throughout the GCL and the hilus of the DG showed weaker stainings of $p27^{Kip1}$ (i.e., $p27^{Kip1+Low}$) (Fig. 5F′, 5G′). Colabeling with NeuN revealed that the $p27^{Kip1+Low}$ cells were postmitotic $NeuN^{+}$ neurons (data not shown) as described previously [38]. Based on the findings by Durand et al. [39], we considered that $Ki\text{-}67^{+}$/$p27^{Kip1+High}$ cells were about to exit the cell cycle. As shown in Figure 5E, the proportion of $Ki\text{-}67^{+}$ precursors that were $p27^{Kip1+High}$ was significantly increased in $Cdk6^{-/-}$ when compared with WT (Fig. 5F–5G″), which is consistent with the above-mentioned data (Fig. 5B–5D). Altogether, these results strongly suggest that Cdk6 controls the cell cycle exit of neuronally committed precursors, thereby regulating the production of postmitotic neurons.

Recently, Lange et al. [40] demonstrated that forcing the lengthening of G_1 is sufficient to promote the exit of the cell cycle of cortical progenitors and their differentiation into projection neurons. As our data support an increased rate of precursor cell cycle exit in $Cdk6^{-/-}$ neurogenic regions, we compared the length of G_1 in Cdk6-knockout and WT animals. To this aim, we performed cumulative S-phase labeling with

BrdU [18, 40] (Fig. 6A–6D). Using this method, we found that the overall duration of the cell cycle (T_C) in DG cycling precursors was increased in Cdk6$^{-/-}$ (22h32′) when compared with WT (19h55′) (Fig. 6J). Importantly, the T_C of WT DG cells presented in this study fits those calculated previously [41, 42]. The maximal BrdU mitotic LI was reached 3 hours after the initial BrdU injection, regardless of the genotype (Fig. 6E–6I), indicating that the combined length of G_2+M phases was comparable in WT and Cdk6$^{-/-}$ DG precursors (Fig. 6J). Conversely, G_1 showed a selective lengthening (+28.08%) in Cdk6$^{-/-}$ when compared with WT controls, whereas S-phase duration was shortened (−8.31%) (Fig. 6J). In accordance with the phenotype observed in the DG, SVZ precursors also showed a significant lengthening of G_1 in the absence of Cdk6 (+82.21%; supporting Information Fig. 8), suggesting Cdk6 as a regulator of G_1 length in both neurogenic niches. Finally, we sought to determine whether this defect was affecting all cycling precursors. Thus, we analyzed BrdU incorporation in immature Neurod1$^-$ and neuronally committed Neurod1$^+$ cycling precursors (i.e., Neurod1$^-$/Ki-67$^+$ and Neurod1$^+$/Ki-67$^+$, respectively) 6 hours after the initial BrdU injection. Interestingly, we first observed that the LI of immature Neurod1$^-$ cells was higher when compared with more committed Neurod1$^+$ cells in WT brains (Fig. 6K). Second, although the LI of Neurod1$^-$ cells remained unchanged, we observed a significant decrease of the LI of Neurod1$^+$ cells in the absence of Cdk6 (Fig. 6K). These results suggest that the overall defect in proliferation observed in the DG of Cdk6-deficient animals mainly results from the impaired proliferation kinetics of neuronally committed precursors.

During cell cycle progression, Cdk6 phosphorylates pRb in G_1, leading to a release of E2f transcription factors and, subsequently, S-phase entry [43]. Similarly to our results, Malumbres et al. [10] previously demonstrated a lengthening of G_1 in Cdk6$^{-/-}$ T lymphocytes on mitogenic stimulation. This defect was concomitant with a delay of pRb phosphorylation on Ser780, a residue specifically targeted by Cdk4/6 [44]. Consequently, we hypothesized that the lengthened G_1 measured in Cdk6$^{-/-}$ neural precursors could partially result from pRb hypophosphorylation. Thus, we microdissected the SVZ of WT and Cdk6$^{-/-}$ mice and carried out western blot analysis. Our results revealed a reduction of the phosphorylation of pRb on Ser780 in Cdk6$^{-/-}$ SVZ precursors (Fig. 6L, 6M). Conversely, in agreement with the absence of proliferation defect in Cdk4$^{-/-}$ brains (Fig. 2), we did not detect any significant difference of pRb phosphorylation on Ser780 in Cdk4$^{-/-}$ SVZ precursors (Fig. 6L, 6N). These observations suggest that: (a) Cdk4 (or any other kinase) cannot compensate efficiently for the lack of Cdk6 pRb-kinase activity in adult neural precursors; (b) the lengthening of G_1 observed in vivo in Cdk6$^{-/-}$ adult neural precursors may arise from a reduced phosphorylation status of pRb.

Seizure-Induced Proliferation and Neurogenesis in Cdk6$^{-/-}$ Mice

Acute seizures have been demonstrated to dramatically induce precursor proliferation in the DG [45–47]. Additionally, a recent report from Varodayan et al. [48] demonstrated that seizure leads to a shortening of the cell cycle in DG precursors, suggesting a link between G_1 phase length and seizure-induced proliferation. To address whether Cdk6 plays a role during seizure-induced proliferation, we injected kainic acid (KA) to WT and Cdk6$^{-/-}$ animals and quantified precursor cell proliferation in the DG 72 hours later, with a protocol that was described previously [49, 50]. Of note, we consistently observed a large overlap between Cdk4/6 and Ki-67 expression 72 hours after either NaCl or KA administration (Supporting Information Fig. 9). As expected (Fig. 2), we found a decreased number of proliferating Ki-67$^+$ cells in NaCl-treated Cdk6$^{-/-}$ when compared with WT brains (Fig. 7A, 7C, 7E). However, our cell countings revealed that the levels of precursor proliferation increased drastically following KA treatment in both genotypes (Fig. 7A–7E). Because seizure has been demonstrated to initially trigger the proliferation of immature/noncommitted precursors [49, 50], we then quantified the numbers of GFAP$^+$/Ki-67$^+$ and Sox2$^+$/Ki-67$^+$ cells following KA injection. We observed a dramatic increase of the number of GFAP$^+$ and Sox2$^+$ proliferating precursors, independently of the mouse genotype (Fig. 7F, 7G). These findings are consistent with our data obtained in basal conditions (Fig. 2) and further confirm that the regulation of immature/noncommitted precursor proliferation and cell cycle kinetics occur in a Cdk6-independent manner. More generally, these data preclude a role for Cdk6 during the initial phase of seizure-induced proliferation. In addition to transiently enhancing cell proliferation, seizures have been shown to increase the production of newborn neurons [51]. Importantly, these newborn neurons exhibit dramatic changes of neuronal polarity and migration, and integrate aberrantly into the pre-existing neuronal network [52–54], leading to long-term structural changes in the hippocampal circuitry that might contribute to chronic epilepsy [55, 56]. To evaluate the consequences of Cdk6 deficiency on seizure-induced neurogenesis, we injected WT and Cdk6$^{-/-}$ animals with BrdU 72 hours following seizure induction and sacrificed the animals 4 weeks later to quantify the number of BrdU$^+$ surviving cells. Consistently with our data obtained in basal conditions, Cdk6-deficiency impaired the production of newborn cells in the epileptic DG (Fig. 7H). Altogether, these data suggest that although KA increases the proliferation of immature/noncommitted Cdk6$^{-/-}$ NPCs to a similar extent as in WT, the absence of Cdk6 largely prevents the burst in neuronal production observed in WT conditions.

Discussion

Our findings demonstrate a unique and crucial role for Cdk6 in controlling neuronally committed precursor expansion and the rate of neuronal production in the adult brain (Supporting Information Fig. 10). Besides, we identified G_1 phase duration as one key regulator of this process.

During brain development, a progressive increase in rates of neuron production is accompanied by increasing frequencies of differentiative divisions that come together with the extension of G_1 phase length [57, 58]. Particularly, proliferative divisions are characterized by a short G_1, whereas differentiative or neurogenic divisions exhibit a longer G_1 [57, 58]. These findings led to the "cell cycle length hypothesis," stating that there is an inverse correlation between G_1 phase duration and the onset of neuronal differentiation [59]. Considering (a) type 1 precursors are mainly slowly dividing and account for a small part of the total proliferative activity of the DG (ref. [60] and the present study) and (b) there is no overlap between the expression of Sox2 and Neurod1 in the DG (refs. [61, 62] and our unpublished observations), the lower LI of Neurod1$^+$ cells when compared with Neurod1$^-$ cells suggests that immature actively proliferating precursors (type 2a) cycle more rapidly than do neuronally committed precursors (types 2b and 3), supporting for the first time the "cell cycle length hypothesis" for adult neurogenic niches. Moreover, the lengthening of G_1 observed in the absence of

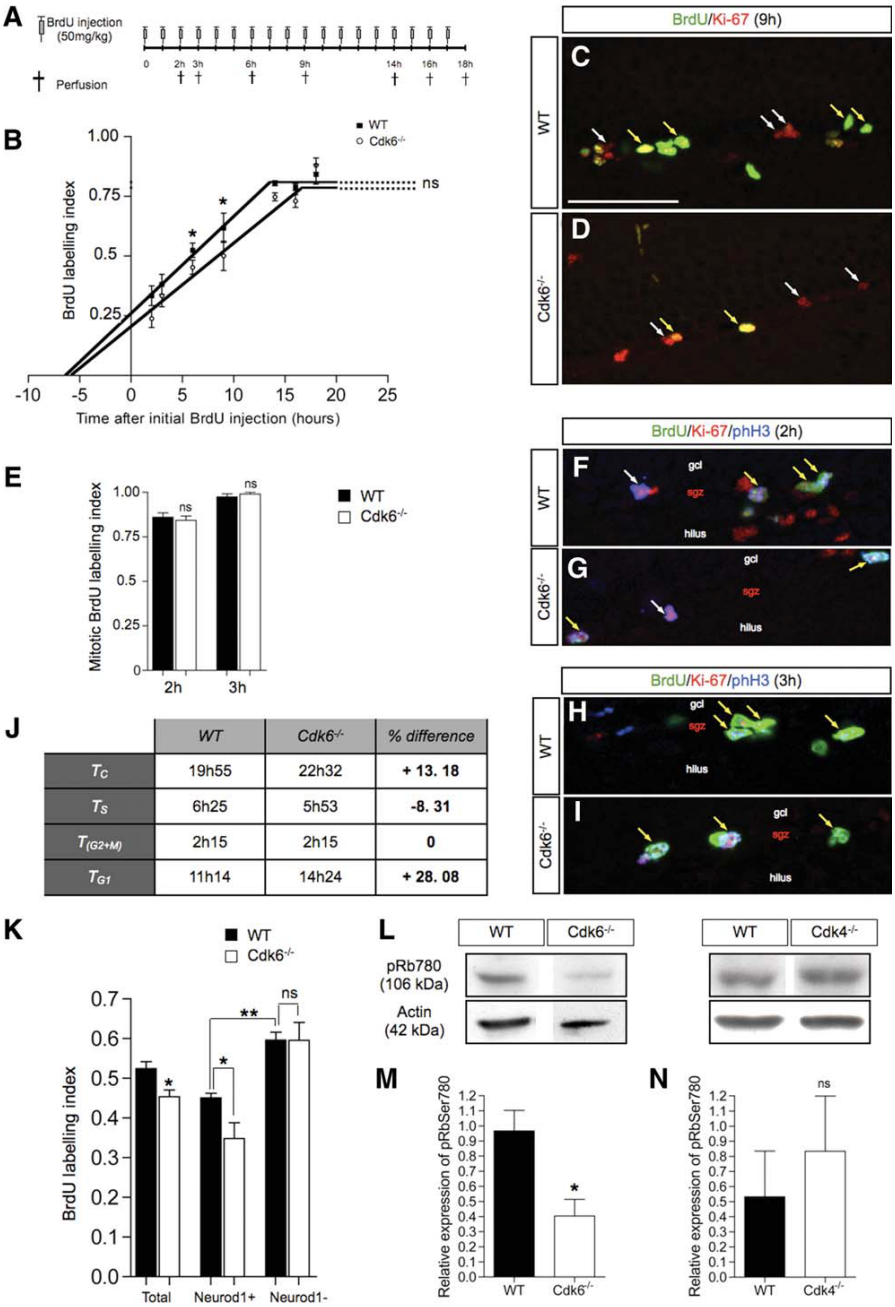

	WT	Cdk6-/-	% difference
T_C	19h55	22h32	+ 13. 18
T_S	6h25	5h53	-8. 31
$T_{(G2+M)}$	2h15	2h15	0
T_{G1}	11h14	14h24	+ 28. 08

Figure 6. Cell cycle kinetics in cyclin-dependent kinase (Cdk) $6^{-/-}$ dentate gyrus (DG). **(A):** Time course of cumulative BrdU labeling in WT and Cdk6$^{-/-}$ DG. BrdU was injected every hour (syringes). Mice were sacrificed (crosses) 2, 3, 6, 9, 14, 16, and 18 hours after the first BrdU injection. **(B):** Cumulative BrdU labeling curves of WT (black squares) and Cdk6$^{-/-}$ (open circles) precursors. Dashed lines indicate growth fractions that were not different between WT and Cdk6$^{-/-}$ animals. **(C, D):** Representative fluorescence images of 1.5 μm thick confocal optical sections of DG stained with BrdU and Ki-67 9 hours after the first BrdU injection in WT **(C)** and Cdk6$^{-/-}$ **(D)** animals. Yellow and white arrows point toward Ki-67^{+}/BrdU^{+} and Ki-67^{+}/BrdU^{-} cells, respectively. **(E):** Mitotic BrdU labeling indices of WT and Cdk6$^{-/-}$ DG after 2 (left) or 3 (right) hours of BrdU exposure. Mitotic labeling index 1.00 = all mitotic (i.e., Ki-67^{+}/phH3^{+}) cells stained with BrdU. **(F–I):** Representative fluorescence images of 1.5 μm thick confocal optical sections stained with BrdU, Ki-67, and phH3, 2 **(F, G)** and 3 **(H, I)** hours after the first BrdU injection in WT **(F, H)** and Cdk6$^{-/-}$ **(G, I)** animals. Yellow and white arrows point toward Ki-67^{+}/BrdU^{+}/phH3^{+} and Ki-67^{+}/BrdU^{-}/phH3^{+} cells, respectively. **(J):** Table showing the total cell cycle time, S-phase, G2 and M phases, and G1 phase duration in WT and Cdk6$^{-/-}$ DG. **(K):** Six-hour BrdU labeling indices of WT (black) and Cdk6$^{-/-}$ (white) precursors among total (left), Neurod1^{+} (middle), and Neurod1^{-} (right) precursors. **(L):** Western blot against pRbSer780 in WT and Cdk6$^{-/-}$ (left), WT and Cdk4$^{-/-}$ (right) subventricular zone precursors. **(M, N):** Histograms showing the corresponding Western blot quantifications. Relative intensity of pRbSer780 signal was calculated by doing the ratio with the actin signal from the same sample. Scale bars = 65 μm **(C, D)**, 55 μm **(F–I)**. Data are the mean of four different animals per genotype per time point ± SD for the cell cycle kinetics analysis **(B, E, J)** and were analyzed by a two-way ANOVA followed by a Bonferroni's post-test **(K)**. Data are the mean of four different animals of each genotype ±SD and were analysed by a Two-way ANOVA followed by a Bonferroni's post-test. **(M, N):** Data are the mean of four proteic extracts coming from four different animals of each genotype ± SD and were analyzed by a Student's *t* test. *,$p < .05$; **, $p < .005$. Abbreviations: BrdU, bromodeoxyuridine; Cdk, cyclin-dependent kinase; gcl: granule cell layer; ns: not significant; sgz: subgranular zone; T_C, total cell cycle time; T_{G2+M}, total G2 and M phases duration, T_{G1}, total G1 phase duration; T_S, total S-phase duration; WT, wild type.

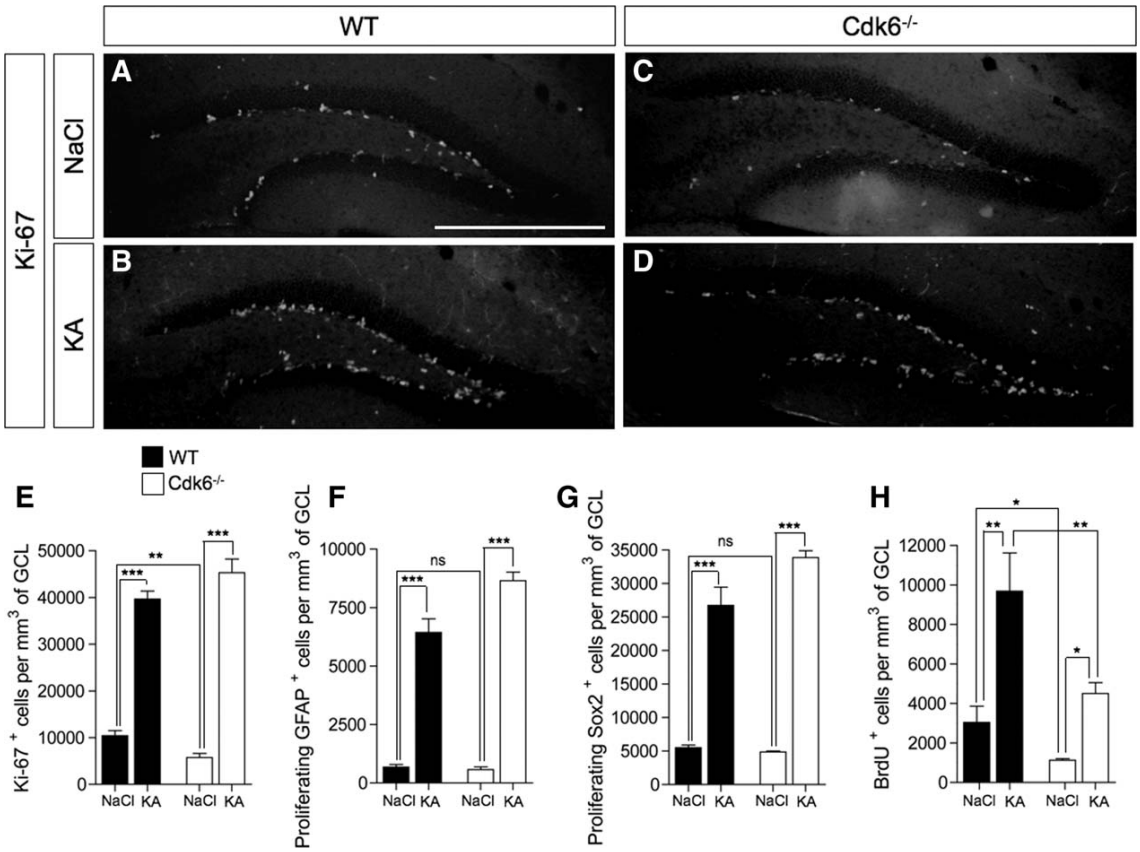

Figure 7. Seizure-induced neurogenesis in wild type (WT) and cyclin-dependent kinase (Cdk) $6^{-/-}$ animals. **(A–D):** Representative fluorescence images of Ki-67 labeling in the dentate gyrus (DG) of saline (NaCl)-WT **(A)** and $Cdk6^{-/-}$ **(C)** and kainic acid (KA)-treated WT **(B)** and $Cdk6^{-/-}$ **(D)** 72 hours after the NaCl or KA injection. **(E–H):** Histograms showing the number of Ki-67^+ cells **(E)**, the number of proliferating (i.e., Ki-67^+)/glial fibrillary acidic protein$^+$ **(F)**, Ki-67^+/Sox2^+ **(G)** cells, and the number of BrdU$^+$ cells 4 weeks after a single BrdU injection (performed 72 hours after the KA injection) **(H)** per mm^3 of granule cell layer in saline- and KA-treated WT and $Cdk6^{-/-}$ DG. Scale bar = 400 μm **(A–D)**. Data are presented as mean ± SD. Statistical analysis were two-way ANOVA followed by a Bonferroni's post-test. **(E-H):** N is four different animals per condition. *, $p < .05$; **, $p < .005$; ***, $p < .001$. Abbreviations: BrdU, bromodeoxyuridine; Cdk, cyclin-dependent kinase; GCL, granule cell layer; GFAP, glial fibrillary acidic protein; KA, kainic acid; ns: not significant; WT, wild type.

Cdk6 causes precocious cell cycle exit and differentiation. Interestingly, as the absence of Cdk6 specifically results in the reduction of both the number and the LI of neuronally committed precursors, one could conceptualize a model where Cdk6, presumably through G_1 length regulation, actively promotes proliferative divisions of type 2b cells, preventing them to prematurely give rise to more differentiated type 3 cells and ultimately to neurons. Furthermore, evidences show that type 3 cells can also divide [15] and the absence of Cdk6 could also interfere with their proliferative capacity. Importantly, we did not detect any defect in immature precursors either in basal nor in seizure induced proliferation, suggesting that Cdk6-independent mechanisms efficiently control their proliferation. However, in contrast with WT animals, the dramatic increase of proliferation we observed in $Cdk6^{-/-}$ mice following KA administration did not lead to a proportional increase of newborn neuron production. These findings suggest that a pharmacological inhibition of Cdk6 may be effective in preventing the production of ectopic granule cell neurons, a putative cause of temporal lobe epilepsy in humans [55, 56]. More generally, our results underline the need to decipher the distinct molecular mechanisms controlling G_1 in the different proliferating populations of the adult brain in normal or pathological conditions.

This work shows that although Cdk4 is expressed in SGZ and SVZ precursors, this kinase is dispensable for cell proliferation in adult neurogenic niches, at least in our experimental conditions. Our results are in accordance with other studies that have previously shown that Cdk4 deficiency does not impede cell proliferation in several highly proliferating tissues, such as skin, small intestine, or hematopoietic system [63, 64]. In addition, Cdk4 is dispensable for liver regeneration following partial hepatectomy [64], an assay considered to be one of the most stringent to evaluate the proliferative capacity of an adult tissue [65]. Altogether, these data support that Cdk4 is, with the exception of certain cell types [9, 19, 66, 67], overall dispensable for adult tissue homeostasis.

Interestingly, we recently demonstrated that another major interphase Cdk, Cdk2, was also dispensable for hippocampal neurogenesis [68]. Importantly, while the long held belief was that all Cdks were expressed in most proliferating cell types [43, 69], we were able to detect Cdk1, Cdk4, and Cdk6 but not Cdk2 expression in the DG and SVZ (our unpublished observations), although a recent article reported a critical role

for the latter in SVZ cell proliferation and self-renewal [70]. Since recent work by Santamaria et al. [71] described a central role for Cdk1 during embryogenesis, it would be interesting to assess if Cdk1 activity also accounts for proliferation in the DG and SVZ as basal levels of both phosphorylation of pRb and cell proliferation are maintained in Cdk6 mutant brains.

Of interest, one major discrepancy between Cdk4 and Cdk6 is the specific role of the latter in blocking differentiation of multiple lineages [69]. For instance, although Cdk4 and Cdk6 are expressed all along the hematopoietic lineage, Cdk6 deficiency specifically impaired expansion of lineage-committed populations rather than proliferation of early hematopoietic precursors [10], a situation mimicking the phenotype we observed in the brain. Interestingly, our results support the idea that the specific involvement of Cdk6 in neural precursors may partially rely on its unique capacity to phosphorylate pRb on Ser780 in these cells. Cdk4$^{-/-}$ embryonic fibroblasts have been previously shown to display reduced levels of pRb-Ser780 while expressing Cdk6 [9], suggesting that the main D-type Cdk responsible for phosphorylation of this residue could be cell-type dependent. Alternatively, it might be conceivable that Cdk4/6 activity itself depends on the cell type [72].

Conclusion

Our work unravels a specific function for the G_1 regulator Cdk6 in the control of adult neurogenesis. More generally, this report is, to our knowledge, the first to show that a modification of G_1 duration influences precursor expansion versus differentiation in an adult tissue and therefore contributes to a better understanding of the mechanisms that underlie the balance between proliferation and differentiation of somatic precursor cells.

Acknowledgments

We thank A. Brose, M. Doupagne, and P. Gengoux for their technical assistance; Drs. K. Yoshikawa and J. Drouin for providing the anti-Dlx2 and anti-Neurod1 antibodies, respectively; Drs. D. Lagace and F. Lallemend for stimulating discussions and valuable comments on the manuscript; the GIGA-Cell Imaging and Flow Cytometry platform for support with confocal microscopy. This work was supported by the Fonds Léon Frédéricq (FLF) and the Fondation Médicale Reine Elisabeth. P.B. was supported by the FLF and a concerted action of the French Community of Belgium (Convention No. 04/09-322). N.C. is a research fellow of the Fonds pour la formation à la Recherche dans l'Industrie et dans l'Agriculture (FRIA). L.N. is funded by the Walloon Excellence in Life Sciences and Biotechnology (WELBIO). L.N. and B.M. are research associate and research director, respectively, from the Belgian Fonds National de la Recherche Scientifique (FNRS). R.V. is currently affiliated with the Department of Cellular and Molecular Medicine, University of Ottawa, Ottawa, ON, Canada.

Disclosure of Potential Conflicts of Interest

The authors indicate no potential conflicts of interest.

References

1 Imayoshi I, Sakamoto M, Ohtsuka T et al. Continuous neurogenesis in the adult brain. Dev Growth Differ 2009;51:379–386.
2 Zetterberg A, Larsson O, Wiman KG. What is the restriction point? Curr Opin Cell Biol 1995;7:835–842.
3 Malumbres M, Barbacid M. Mammalian cyclin-dependent kinases. Trends Biochem Sci 2005;30:630–641.
4 Malumbres M, Barbacid M. Cell cycle, cdks and cancer: A changing paradigm. Nat Rev Cancer 2009;9:153–166.
5 Satyanarayana A, Kaldis P. Mammalian cell-cycle regulation: Several Cdks, numerous cyclins and diverse compensatory mechanisms. Oncogene 2009;28:2925–2939.
6 Sherr CJ, Roberts JM. Inhibitors of mammalian G1 cyclin-dependent kinases. Genes Dev 1995;9:1149–1163.
7 Doetsch F, Verdugo JM, Caille I et al. Lack of the cell-cycle inhibitor p27Kip1 results in selective increase of transit-amplifying cells for adult neurogenesis. J Neurosci 2002;22:2255–2264.
8 Kowalczyk A, Filipkowski RK, Rylski M et al. The critical role of cyclin D2 in adult neurogenesis. J Cell Biol 2004;167:209–213.
9 Tsutsui T, Hesabi B, Moons DS et al. Targeted disruption of CDK4 delays cell cycle entry with enhanced p27(Kip1) activity. Mol Cell Biol 1999;19:7011–7019.
10 Malumbres M, Sotillo R, Santamaria D et al. Mammalian cells cycle without the D-type cyclin-dependent kinases Cdk4 and Cdk6. Cell 2004;118:493–504.
11 Vanderluit JL, Wylie CA, McClellan KA et al. The retinoblastoma family member p107 regulates the rate of progenitor commitment to a neuronal fate. J Cell Biol 2007;178:129–139.
12 Kim WR, Kim Y, Eun B et al. Impaired migration in the rostral migratory stream but spared olfactory function after the elimination of programmed cell death in Bax knock-out mice. J Neurosci 2007;27:14392–14403.
13 del Valle K, Theus MH, Bethea JR et al. Neural progenitors proliferation is inhibited by EphB3 in the developing subventricular zone. Int J Dev Neurosci 2011;29:9–14.
14 Li L, Walker TL, Zhang Y et al. Endogenous interferon gamma directly regulates neural precursors in the non-inflammatory brain. J Neurosci 2010;30:9038–9050.
15 Steiner B, Zurborg S, Horster H et al. Differential 24 h responsiveness of Prox1-expressing precursor cells in adult hippocampal neurogenesis to physical activity, environmental enrichment, and kainic acid-induced seizures. Neuroscience 2008;154:521–529.
16 Scholzen T, Gerdes J. The Ki-67 protein: From the known and the unknown. J Cell Physiol 2000;182:311–322.
17 Pilaz LJ, Patti D, Marcy G et al. Forced G1-phase reduction alters mode of division, neuron number, and laminar phenotype in the cerebral cortex. Proc Natl Acad Sci USA 2009;106:21924–21929.
18 Takahashi T, Nowakowski RS, Caviness VS, Jr. Cell cycle parameters and patterns of nuclear movement in the neocortical proliferative zone of the fetal mouse. J Neurosci 1993;13:820–833.
19 Rane SG, Dubus P, Mettus RV et al. Loss of Cdk4 expression causes insulin-deficient diabetes and Cdk4 activation results in beta-islet cell hyperplasia. Nature Genetics 1999;22:44–52.
20 Kempermann G, Kuhn HG, Gage FH. Genetic influence on neurogenesis in the dentate gyrus of adult mice. Proc Natl Acad Sci USA 1997;94:10409–10414.
21 Couillard-Despres S, Winner B, Schaubeck S et al. Doublecortin expression levels in adult brain reflect neurogenesis. Eur J Neurosci 2005;21:1–14.
22 Biebl M, Cooper CM, Winkler J et al. Analysis of neurogenesis and programmed cell death reveals a self-renewing capacity in the adult rat brain. Neurosci Lett 2000;291:17–20.
23 Kempermann G, Jessberger S, Steiner B et al. Milestones of neuronal development in the adult hippocampus. Trends Neurosci 2004;27:447–452.
24 Encinas JM, Vaahtokari A, Enikolopov G. Fluoxetine targets early progenitor cells in the adult brain. Proc Natl Acad Sci USA 2006;103:8233–8238.
25 Suh H, Consiglio A, Ray J et al. In vivo fate analysis reveals the multipotent and self-renewal capacities of Sox2+ neural stem cells in the adult hippocampus. Cell Stem Cell 2007;1:515–528.
26 Roybon L, Hjalt T, Stott S et al. Neurogenin2 directs granule neuroblast production and amplification while NeuroD1 specifies neuronal fate during hippocampal neurogenesis. PLoS One 2009;4:e4779.

27 Hodge RD, Kowalczyk TD, Wolf SA et al. Intermediate progenitors in adult hippocampal neurogenesis: Tbr2 expression and coordinate regulation of neuronal output. J Neurosci 2008;28:3707–3717.
28 Kriegstein A, Alvarez-Buylla A. The glial nature of embryonic and adult neural stem cells. Annu Rev Neurosci 2009;32:149–184.
29 Ghashghaei HT, Weber J, Pevny L et al. The role of neuregulin-ErbB4 interactions on the proliferation and organization of cells in the subventricular zone. Proc Natl Acad Sci USA 2006;103:1930–1935.
30 Doetsch F, Garcia-Verdugo JM, Alvarez-Buylla A. Cellular composition and three-dimensional organization of the subventricular germinal zone in the adult mammalian brain. J Neurosci 1997;17:5046–5061.
31 Pastrana E, Cheng LC, Doetsch F. Simultaneous prospective purification of adult subventricular zone neural stem cells and their progeny. Proc Natl Acad Sci USA 2009;106:6387–6392.
32 Whitman MC, Greer CA. Adult neurogenesis and the olfactory system. Prog Neurobiol 2009;89:162–175.
33 Mizrahi A. Dendritic development and plasticity of adult-born neurons in the mouse olfactory bulb. Nat Neurosci 2007;10:444–452.
34 Cheng LC, Pastrana E, Tavazoie M et al. miR-124 regulates adult neurogenesis in the subventricular zone stem cell niche. Nat Neurosci 2009;12:399–408.
35 Woodhead GJ, Mutch CA, Olson EC et al. Cell-autonomous beta-catenin signaling regulates cortical precursor proliferation. J Neurosci 2006;26:12620–12630.
36 Inoue T, Ota M, Ogawa M et al. Zic1 and Zic3 regulate medial forebrain development through expansion of neuronal progenitors. J Neurosci 2007;27:5461–5473.
37 Glickstein SB, Monaghan JA, Koeller HB et al. Cyclin D2 is critical for intermediate progenitor cell proliferation in the embryonic cortex. J Neurosci 2009;29:9614–9624.
38 Breunig JJ, Silbereis J, Vaccarino FM et al. Notch regulates cell fate and dendrite morphology of newborn neurons in the postnatal dentate gyrus. Proc Natl Acad Sci USA 2007;104:20558–20563.
39 Durand B, Gao FB, Raff M. Accumulation of the cyclin-dependent kinase inhibitor p27/Kip1 and the timing of oligodendrocyte differentiation. EMBO J 1997;16:306–317.
40 Lange C, Huttner WB, Calegari F. Cdk4/cyclinD1 overexpression in neural stem cells shortens G1, delays neurogenesis, and promotes the generation and expansion of basal progenitors. Cell Stem Cell 2009;5:320–331.
41 Hayes NL, Nowakowski RS. Dynamics of cell proliferation in the adult dentate gyrus of two inbred strains of mice. Brain Res Dev Brain Res 2002;134:77–85.
42 Mandyam CD, Harburg GC, Eisch AJ. Determination of key aspects of precursor cell proliferation, cell cycle length and kinetics in the adult mouse subgranular zone. Neuroscience 2007;146:108–122.
43 Meyerson M, Harlow E. Identification of G1 kinase activity for cdk6, a novel cyclin D partner. Mol Cell Biol 1994;14:2077–2086.
44 Kitagawa M, Higashi H, Jung HK et al. The consensus motif for phosphorylation by cyclin D1-Cdk4 is different from that for phosphorylation by cyclin A/E-Cdk2. EMBO J 1996;15:7060–7069.
45 Parent JM, Yu TW, Leibowitz RT et al. Dentate granule cell neurogenesis is increased by seizures and contributes to aberrant network reorganization in the adult rat hippocampus. J Neurosci 1997;17:3727–3738.
46 Bengzon J, Kokaia Z, Elmer E et al. Apoptosis and proliferation of dentate gyrus neurons after single and intermittent limbic seizures. Proc Natl Acad Sci USA 1997;94:10432–10437.
47 Parent JM, Janumpalli S, McNamara JO et al. Increased dentate granule cell neurogenesis following amygdala kindling in the adult rat. Neurosci Lett 1998;247:9–12.
48 Varodayan FP, Zhu XJ, Cui XN et al. Seizures increase cell proliferation in the dentate gyrus by shortening progenitor cell-cycle length. Epilepsia 2009;50:2638–2647.
49 Huttmann K, Sadgrove M, Wallraff A et al. Seizures preferentially stimulate proliferation of radial glia-like astrocytes in the adult dentate gyrus: Functional and immunocytochemical analysis. Eur J Neurosci 2003;18:2769–2778.
50 Lugert S, Basak O, Knuckles P et al. Quiescent and active hippocampal neural stem cells with distinct morphologies respond selectively to physiological and pathological stimuli and aging. Cell Stem Cell 2010;6:445–456.
51 Jessberger S, Romer B, Babu H et al. Seizures induce proliferation and dispersion of doublecortin-positive hippocampal progenitor cells. Exp Neurol 2005;196:342–351.
52 Shapiro LA, Ribak CE. Newly born dentate granule neurons after pilocarpine-induced epilepsy have hilar basal dendrites with immature synapses. Epilepsy Res 2006;69:53–66.
53 Jessberger S, Zhao C, Toni N et al. Seizure-associated, aberrant neurogenesis in adult rats characterized with retrovirus-mediated cell labeling. J Neurosci 2007;27:9400–9407.
54 Overstreet-Wadiche LS, Bromberg DA, Bensen AL et al. Seizures accelerate functional integration of adult-generated granule cells. J Neurosci 2006;26:4095–4103.
55 Parent JM. The role of seizure-induced neurogenesis in epileptogenesis and brain repair. Epilepsy Res 2002;50:179–189.
56 Jakubs K, Nanobashvili A, Bonde S et al. Environment matters: Synaptic properties of neurons born in the epileptic adult brain develop to reduce excitability. Neuron 2006;52:1047–1059.
57 Dehay C, Kennedy H. Cell-cycle control and cortical development. Nat Rev Neurosci 2007;8:438–450.
58 Salomoni P, Calegari F. Cell cycle control of mammalian neural stem cells: Putting a speed limit on G1. Trends Cell Biol 2010;20:233–243.
59 Calegari F, Huttner WB. An inhibition of cyclin-dependent kinases that lengthens, but does not arrest, neuroepithelial cell cycle induces premature neurogenesis. J Cell Sci 2003;116:4947–4955.
60 Kronenberg G, Reuter K, Steiner B et al. Subpopulations of proliferating cells of the adult hippocampus respond differently to physiologic neurogenic stimuli. J Comp Neurol 2003;467:455–463.
61 Kuwabara T, Hsieh J, Muotri A et al. Wnt-mediated activation of NeuroD1 and retro-elements during adult neurogenesis. Nat Neurosci 2009;12:1097–1105.
62 Gao Z, Ure K, Ables JL et al. Neurod1 is essential for the survival and maturation of adult-born neurons. Nat Neurosci 2009;12:1090–1092.
63 Rodriguez-Puebla ML, Miliani de Marval PL, LaCava M et al. Cdk4 deficiency inhibits skin tumor development but does not affect normal keratinocyte proliferation. Am J Pathol 2002;161:405–411.
64 Barriere C, Santamaria D, Cerqueira A et al. Mice thrive without Cdk4 and Cdk2. Mol Oncol 2007;1:72–83.
65 Duncan AW, Dorrell C, Grompe M. Stem cells and liver regeneration. Gastroenterology 2009;137:466–481.
66 Atanasoski S, Boentert M, De Ventura L et al. Postnatal Schwann cell proliferation but not myelination is strictly and uniquely dependent on cyclin-dependent kinase 4 (cdk4). Mol Cell Neurosci 2008;37:519–527.
67 Jirawatnotai S, Aziyu A, Osmundson EC et al. Cdk4 is indispensable for postnatal proliferation of the anterior pituitary. J Biol Chem 2004;279:51100–51106.
68 Vandenbosch R, Borgs L, Beukelaers P et al. CDK2 is dispensable for adult hippocampal neurogenesis. Cell Cycle 2007;6:3065–3069.
69 Grossel MJ, Hinds PW. Beyond the cell cycle: A new role for Cdk6 in differentiation. J Cell Biochem 2006;97:485–493.
70 Jablonska B, Aguirre A, Vandenbosch R et al. Cdk2 is critical for proliferation and self-renewal of neural progenitor cells in the adult subventricular zone. J Cell Biol 2007;179:1231–1245.
71 Santamaria D, Barriere C, Cerqueira A et al. Cdk1 is sufficient to drive the mammalian cell cycle. Nature 2007;448:811–815.
72 Bockstaele L, Bisteau X, Paternot S et al. Differential regulation of cyclin-dependent kinase 4 (CDK4) and CDK6, evidence that CDK4 might not be activated by CDK7, and design of a CDK6 activating mutation. Mol Cell Biol 2009;29:4188–4200.


See www.StemCells.com for supporting information available online.